

THERMAL ANALYSIS ON NATURAL-CONVECTION COUPLED WITH RADIATIVE HEAT TRANSFER IN A SATURATED POROUS CAVITY

by

Yuanyuan CHEN*, **Yiwei CHEN**, and **Xuecheng XU**

State Key Laboratory of Refractories and Metallurgy,
Wuhan University of Science and Technology, Wuhan, China

Original scientific paper
<https://doi.org/10.2298/TSCI210309256C>

Porous foam is an ideal material for enhancing radiative heat transfer in numerous thermal equipment. The solid skeletons of porous foams can absorb/release radiative energy and transfer convective energy with the surrounding fluid in the pores. In this paper, the conduction-convection-radiation coupling heat transfer in a porous cavity is investigated. A local thermal non-equilibrium model is used to represent the energy transport during the solid and fluid phases. The heat flux caused by thermal radiation is obtained by solving the radiation transfer equation. The thermal and fluid fields are studied to discern various parameters, including the Planck numbers, the modified Rayleigh numbers, and the interphase heat transfer coefficients, H . Our study indicates the following: the effect of radiation can be neglected when $Pl > 20$, the modified Rayleigh numbers have little influence on the solid temperature when the radiative heat transfer is dominant and the convective heat transfer between the two-phases is weak, and the local thermal-equilibrium can be formed when H exhibits high values.

Key words: coupled heat transfer; porous cavity; local thermal non-equilibrium, numerical analysis, radiative transfer equation

Introduction

Metal and ceramic foams play an important role in various industrial applications because they have attractive thermal mechanical properties, including high porosity, high surface area and volume ratios, and the ability to mix and pass fluids [1, 2]. A system composed of a solid skeleton and pores occupied by fluid is the main structural feature, which can be regarded as a semitransparent medium [3]. When they are used in a high temperature environment, the solid skeletons of porous foams can absorb/release radiative energy and transfer convective energy with surrounding fluid in the pores. In other words, conduction-convection-radiation integrated heat transfer will occur. Therefore, in many fields, porous foam is an ideal material for enhancing combined heat transfer of convection and radiation, such as porous media combustion [4], fire barriers [5], solar energy technology [6], and heat porous exchangers [7, 8]. In the design of these systems, it is important to understand the complex coupled heat transfer process. To this end, much work has been done in the past few decades. In the study of heat transfer inside porous media, there are two main models that are widely used, namely, the local thermal equilibrium (LTE) model and the local thermal imbalance (LTNE) model. Many works have focused on the effect of radiation on heat transfer in porous media using the Rosseland diffusion

* Corresponding author, e-mail: chenyuanyuan@wust.edu.cn

assumption and the LTE model. Astanina *et al.* [9] studied the natural-convection combined with thermal radiation inside a square porous cavity filled with a fluid of temperature-dependent viscosity. Sheikholeslami and Shehzad [10] studied the effect of thermal radiation on the heat transfer of a nanofluid in a porous enclosure. Their results demonstrated that the Nusselt number is directly related to the radiation parameter. The convection was enhanced with the increase in the radiation parameter. Shateria and Salahshour [11] studied the temperature distribution and thermal performance of convective-radiative porous fins. They showed that the fin efficiency was improved with the increase in the conductive-radiative parameter. Chen *et al.* [12] studied the non-linear heat transfer in a porous plate with convective and radiative boundary conditions. Their results indicated that the dimensionless temperature increased with increasing Rosseland parameters. Ghalambaz *et al.* [13] studied the effect of radiation on natural-convection heat transfer in a square porous cavity saturated with a nanofluid. Their results indicated that the presence of radiation reduces the temperature gradient but increases the thermal diffusion in the porous media. The overall effect of the presence of radiation was to increase the heat transfer. Jamal-Abad *et al.* [14] studied convective-radiative heat transfer in a porous air heater heated by solar. They found that the heater's efficiency is improved with the increase of the radiation parameter. Lopez *et al.* [15] numerically investigated the MHD flow through a vertical porous micro-channel. The conjugate convective-radiative heat transfer on the boundary was used to solve and analyzed the heat transfer affected by non-linear thermal radiation. The results proved that the generation of global entropy increases with the increasing of radiation parameter. Barnoon *et al.* [16] investigated the natural-convection of a non-Newtonian nanofluid in a cylindrical porous cavity with and without thermal radiation effect. They found that considering the effects of thermal radiation, the heat transfer is expected to be lower than that which does not exist. Arafa *et al.* [17] examined an unsteady convection-radiation interaction flow of power-law non-Newtonian nanofluids within inclined porous enclosures. Ajibade *et al.* [18] investigated the effect of dynamic viscosity and non-linear thermal radiation on free convective flow through a vertical porous channel. The results showed that the use of linear radiation undermined the flow characteristics. Olajuwon [19] numerically investigated the convection heat transfer in a hydromagnetic Carreau fluid past a vertical porous plate in presence of thermal radiation. Izadi [20] studied the MHD thermogravitational convection and thermal radiation of a micropolar nanoliquid in a porous chamber. They found that a rise of the thermal radiation parameter illustrates a growth of both average Nusselt number and nanofluid circulation intensity.

In the aforementioned studies, the Rosseland approximation was used to simplify the solution of radiative transfer, and it is well known that the Rosseland approximation is reasonable only in the case of optical thick media. To obtain more accurate heat flux radiated by the solid skeleton and to study the heat transfer in more complex radiation participating media, we need to solve the radiative transfer equation (RTE). For these purposes, Talukdar *et al.* [21] numerically studied the coupled radiative-convective heat transfer in a porous medium bounded by two parallel grey plates with constant temperature. The influences of the conduction and radiation interactive parameters, extinction coefficients, scattering albedo, and wall emissivity on the Nusselt numbers and thermal field were investigated. Abdesslem *et al.* [22] numerically investigated a transient coupled convection-radiation heat transfer in porous beds saturated with an isotropic and homogeneous fluid. The influences of radiation characteristics, for instance the scattering coefficients, scattering albedo and absorption coefficients, on flow and thermal transfer behaviours in porous medium were studied. Elgazery [23] numerically investigated the influences of radiative characteristics on an unsteady natural convective heat transfer in the porous medium saturated with non-Newtonian fluid.

In porous medium, the temperature differences between the solid skeleton and fluid can be ignored in the event of sufficient heat transfer between the two-phases, and then the single energy equation model based on the LTE assumption is valid. Otherwise, the LTNE model must be used. Especially in the applications under high temperature, thermal radiation absorbed/emitted by the solid skeletons may cause an abundant heat transfer between the two-phases in the porous medium. Research on the LTNE model with radiation from an RTE solution in porous media is still limited. There are few studies in this area. Chen *et al.* [24] analyzed the transient radiation and convection coupled heat transfer in porous tube exchangers with high temperature. The effects of the average particle diameters, porosities, inlet fluid velocities, and solid skeletons thermal conductivities on the temperature difference were analysed. Mahmoudi [25] studied the influences of thermal radiation from the solid phase on thermal fields in porous pipes under a forced convective heat transfer process. The effect of radiation on the thermal field was analysed by the Darcy number, inertia parameter, porosity and thermal conductivity ratio. The discrete ordinate method was used to get the heat flux of radiation. They found that neglecting radiation of the solid skeleton will lead to significant errors in predicting the solid skeleton and fluid temperatures. Chen *et al.* [24] numerically investigated the transient thermal performance of coupled radiative and convective heat transfer in a circular tube exchanger filled with porous material. The Monte-Carlo method is used to solve the radiative heat transfer. Mesgarpour [26] investigated the effect on the temperature of a new model of the porous fin as rows of connected sphere. To increase accuracy in the calculations, the thermal radiation was examined by solving the RTE.

It is apparent from this literature investigation and our collective knowledge that the conduction-convection heat transfer, together with the influences of thermal radiation on local thermal non-equilibrium problems in porous media, is not fully understood. In this paper, the conduction-convection-radiation combined heat transfer in a square porous cavity is numerically studied using the Chebyshev collocation spectral method (CCSM). The effect of the Rayleigh numbers, Planck numbers, inter-phases heat transfer coefficients and thermal conductivity ratios on the flow and thermal field, Nusselt numbers have been investigated.

Governing equations and geometrical configuration

To formulate the problem, we consider a saturated porous cavity with a Newtonian fluid as shown in fig. 1. The fluid-flow is assumed to be a Boussinesq one and represented by the Darcy flow model. The right vertical wall of the cavity is isothermally hot, while the left wall is isothermally cold, and the horizontal walls of the cavity are adiabatic. The four walls are grey diffuse surfaces with constant emissivities and reflectivities. The solid phase of the porous media is assumed to be gray, emitting, absorbing and isotropic scattering media. The fluid is considered to be non-radiative in comparison solid radiation [27]. The two-phases exist everywhere in local thermal non-equilibrium. Based on the dimensional form of the governing equations from [28, 29], using the variable transformation as eq. (1), the governing dimensionless equations can be obtained:

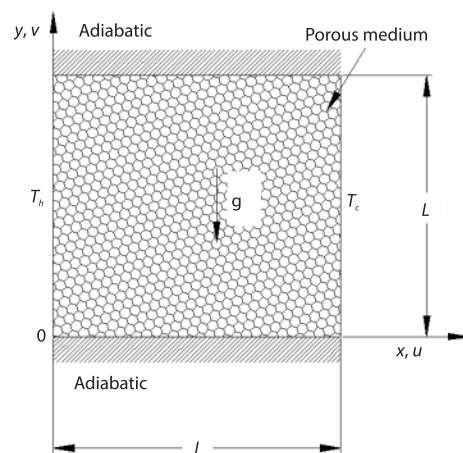


Figure 1. Schematic diagram for the physical and co-ordinate system

Based on the variable transformation as eq. (1), the governing dimensionless equations can be obtained:

$$X = \frac{x}{L}, Y = \frac{y}{L}, S = \frac{s}{L}, U = \frac{uL}{(\rho c_p)_f / \lambda_f}, V = \frac{vL}{(\rho c_p)_f / \lambda_f}$$

$$T_0 = \frac{T_h + T_c}{2}, \theta_s = \frac{T_s - T_0}{T_h - T_c}, \theta_f = \frac{T_f - T_0}{T_h - T_c}, \delta = \frac{T_h - T_c}{T_0}, J = \frac{\pi I}{\sigma T_0^4}, \Theta = \theta_s \delta + 1 \quad (1)$$

$$G = \int_{4\pi} \frac{J}{\pi} d\Omega, \beta = \kappa_a + \kappa_s, \omega = \frac{\kappa_s}{\beta}, \tau_L = \beta L$$

$$\frac{\partial \Psi}{\partial t} - \text{Ra} \frac{\partial \theta_f}{\partial X} = \frac{\partial^2 \Psi}{\partial X^2} + \frac{\partial^2 \Psi}{\partial Y^2} \quad (2)$$

$$\frac{\partial \theta_f}{\partial t} + \frac{\partial \Psi}{\partial Y} \frac{\partial \theta_f}{\partial X} - \frac{\partial \Psi}{\partial X} \frac{\partial \theta_f}{\partial Y} = \frac{\partial^2 \theta_f}{\partial X^2} + \frac{\partial^2 \theta_f}{\partial Y^2} + H(\theta_s - \theta_f) \quad (3)$$

$$\zeta \frac{\partial \theta_s}{\partial t} = \frac{\partial^2 \theta_s}{\partial X^2} + \frac{\partial^2 \theta_s}{\partial Y^2} + \gamma H(\theta_f - \theta_s) - \frac{\tau_L(1-\omega)}{\delta \text{Pl}} \left(\Theta^4 - \frac{G}{4} \right) \quad (4)$$

$$\frac{dJ(\mathbf{r}, \Omega)}{\tau_L dS} = (1-\omega)\Theta^4 - J(\mathbf{r}, \Omega) + \frac{\omega}{4\pi} \int_{4\pi} J(\mathbf{r}, \bar{\Omega}) \Phi(\Omega, \bar{\Omega}) d\bar{\Omega} \quad (5)$$

where Ra is the modified Rayleigh numbers, Pl – the Planck numbers, H – the interphase heat transfer coefficients, γ – the ratios of thermal conductivity, ζ – the ratios of thermal diffusivity and Ψ – the stream function, which are given:

$$\text{Ra} = \frac{gK\alpha_V(T_h - T_c)L}{\nu\lambda_f / (\rho c_p)_f}, \text{Pl} = \frac{\lambda_s / L}{4\sigma T_0^3}, H = \frac{hL^2}{\phi\lambda_f}, \gamma = \frac{\phi\lambda_f}{(1-\phi)\lambda_s}, \zeta = \frac{\lambda_f / (\rho c_p)_f}{\lambda_s / (\rho c_p)_s} \quad (6)$$

$$U = \frac{\partial \Psi}{\partial Y}, V = -\frac{\partial \Psi}{\partial X}$$

The boundary conditions together with the initial conditions in the dimensionless forms:

$$\begin{aligned} &\text{for } t = 0: \Psi = \theta_f = \theta_s = J = 0 \\ &\text{for } t > 0: \Psi(0, Y) = \Psi(1, Y) = \Psi(X, 0) = \Psi(X, 1) = 0 \\ &\theta_f(1, Y) = \theta_s(1, Y) = -0.5, \theta_f(0, Y) = \theta_s(0, Y) = 0.5 \\ &-\frac{\partial \theta_s}{\partial Y} \Big|_{Y=0,1} + \frac{\varepsilon_w}{4\text{Pl}\delta} \left(\Theta_{sw}^4 - \int_{\mathbf{n}_w \cdot \bar{\Omega} < 0} J(r_w, \bar{\Omega}) |\mathbf{n}_w \cdot \bar{\Omega}| d\bar{\Omega} \right) = 0 \\ &\frac{\partial \theta_f}{\partial Y} \Big|_{Y=0,1} = 0 \end{aligned} \quad (7)$$

The boundary condition for eq. (5):

$$J(\mathbf{r}_w, \Omega) = \varepsilon_w \Theta_w^4 + \frac{1-\varepsilon_w}{\pi} \int_{\mathbf{n}_w \cdot \bar{\Omega} < 0} J(\mathbf{r}_w, \bar{\Omega}) |\mathbf{n}_w \cdot \bar{\Omega}| d\bar{\Omega}, \quad \mathbf{n}_w \cdot \bar{\Omega} < 0 \quad (8)$$

Numerical solution and validation

Numerical solution

The time derivatives of the PDE are discretized by a semi-implicit scheme with finite difference approximation. The time step is $\Delta t = 10^{-6}$, which satisfies the Courant-Friedrichs-Lewy condition. The CCSM is used for the spatial discretization of PDE. The Chebyshev Gauss Lobatto collocation point is selected. All the governing equations are solved on one same grid system. The detailed numerical method of the governing equations and the solve method of the matrix can be found in our previous work [28]. The convergence error is set to be 10^{-6} . The MATLAB has been used to develop the implementation codes. After obtaining the temperature field and radiative intensity, the convective heat fluxes of the fluid phase, the conductive and radiative heat fluxes of the solid phase in dimensionless forms on the walls can be obtained:

$$\begin{aligned} \text{Nu}^{\text{COV}} &= \frac{q^{\text{COV}} L}{\lambda_f (T_h - T_c)} \Big|_{X=0,1} = -\frac{d\theta_f}{dX} \Big|_{X=0,1} \\ \text{Nu}^{\text{COD}} &= \frac{q^{\text{COD}} L}{\lambda_s (T_h - T_c)} \Big|_{X=0,1} = -\frac{d\theta_s}{dX} \Big|_{X=0,1} \\ \text{Nu}^{\text{R}} &= \frac{1}{4\text{Pl}\delta} \frac{q^{\text{R}}}{\sigma T_0^4} \Big|_{X=0,1} = \frac{1}{4\text{Pl}\delta} \varepsilon_w \left(\Theta^4 - \frac{1}{\pi} \int \tilde{J} d\Omega \right) \Big|_{X=0,1} \end{aligned} \tag{9}$$

The corresponding total average Nusselt numbers on the hot wall is defined:

$$\overline{\text{Nu}}_h^T = \int_0^1 \text{Nu}_h^T dY = \int_0^1 \text{Nu}_h^{\text{COV}} + \int_0^1 \text{Nu}_h^{\text{COD}} + \int_0^1 \text{Nu}_h^{\text{R}} = \overline{\text{Nu}}_h^{\text{COV}} + \overline{\text{Nu}}_h^{\text{COD}} + \overline{\text{Nu}}_h^{\text{R}} \tag{10}$$

Code validation

In order to find out the grid independency, three grid systems are considered and they are 24×24 , 44×44 , and 64×64 . As seen in tab. 1, the uniform grid of 44×44 points has been selected for the following analysis for any increase beyond a set of 44×44 results in a change of average Nusselt number less than 0.167%. Table 2 compare the accuracy of the average Nusselt number for different values of the Rayleigh number with some numerical solutions reported by different authors without radiation under LTE assumption. It is seen from these tables that the agreement between the present and the previous results is excellent. Furthermore, the validation of radiation transfer in a 2-D cavity occupied by grey scattering media was verified in preliminary work of our team [30]. This validation will not be repeated here.

Table 1. Average Nusselt numbers at different grid numbers for $\text{Ra} = 1000, H = 10, \gamma = 1, \text{Pl} = 0.02, \tau_L = 1.0, \omega = 0.5,$ and $\varepsilon_w = 0.6$

Parameters	Grid numbers		
	64×64	44×44	24×24
$\overline{\text{Nu}}_h^{\text{COV}}$	12.2368	12.2565	12.6684
$\overline{\text{Nu}}_h^{\text{R}}$	15.6989	15.6967	15.6870

Table 2. Comparison of average Nusselt number with some previous numerical results

Authors	Ra		
	10	100	1000
[31]		3. 118	13. 637
[32]	1. 065	2. 801	
[29]	1. 079	3. 160	14. 060
Present results	1. 073	3. 116	13. 692

Results and discussions

Different modified Rayleigh and Planck numbers, and interphase heat transfer coefficients H on the fluid-flow and heat transfer in the porous cavity are numerically investigated, according to the reference [26, 29, 31]. The discussions hereafter are valid with $\tau_L = 1.0$, $\omega = 0.5$, and $\varepsilon_w = 0.6$. Numerical results are presented by means of streamlines and isotherms.

Effect of modified rayleigh number

Figure 2 shows the effect of different Rayleigh number on the streamlines and isotherms in the cavity while $H = 10$, $\gamma = 1.0$, and $PI = 0.02$. The streamlines rise along the hot wall and descends along the cold wall, which presents a circulating cell pattern. Due to different radiative absorption ratios, the structure of the cell in the cavity is asymmetrical, and the fluid-flow is stronger near the cold wall. With the increase in Rayleigh number, the flow in the cavity is significantly enhanced, and the streamlines are accelerated by gathering to the cold wall. The fluid isotherms are greatly influenced by Rayleigh number. When $Ra = 10$, the fluid isotherms are nearly parallel to the vertical walls, which means that the convection effect is small, and the heat transfer is dominated mainly by conduction and radiation. As Rayleigh number increases, the fluid isotherms begin to twist, the upper parts of the isotherms gather towards the cold wall quickly, and the lower parts of the isotherms gather towards the hot wall more slowly, so the heat transfer rate near the upper cold wall is strengthened. The effect of Rayleigh number on the solid isotherms is not obvious because the radiation between the solid phases is high when $PI = 0.02$. Meanwhile, the interphase heat transfer coefficient is small ($H = 10$), so the changes in fluid temperature have a relatively small effect on the solid temperature. At this moment, the radiation heat transfer determines the distribution of the solid isotherms.

Effect of Planck number

The Planck number represents the ratio of the conduction heat transfer to the radiation heat transfer. As Planck number increases, the proportion of radiation decreases. The influence of Planck number on the flow and heat transfer are demonstrated in fig. 3. The other parameters are set as $Ra = 1000$, $H = 10$, and $\gamma = 0$. As shown in this figure, the increase in Planck number gradually changes the cell shape from asymmetrical to symmetrical. The streamlines and the isotherms are very similar between $PI = 20$ and without-radiation, meaning when the value of Planck number is bigger than 20, the effect of radiation can be neglected. Meanwhile, when $PI = 0.02$, the solid isotherms greater than zero occupy three-quarters of the space of the cavity, and they are almost parallel to the vertical walls. The heat transfer near the cold wall is stronger because the temperature gradient near the cold wall is larger. When Planck number increases, the effect of radiation weakens, and then the convection makes the solid isotherms begin to distort. The fluid isotherms do not change significantly with the Planck number, because the the fluid radiation is neglect and the interphase heat transfer coefficient between two-phases is small ($H = 10$). When Planck number increases, the fluid isotherms slightly gather to the lower part of the hot wall and the upper part of the cold wall, thus increasing temperature gradient at corresponding position and strengthening the flow.

Effect of the Interphase heat transfer coefficients

Figure 4 shows the effect of the interphase heat transfer coefficients on the flow and thermal field in the cavity. The interphase heat transfer coefficients are set to be $H = 0.1$,

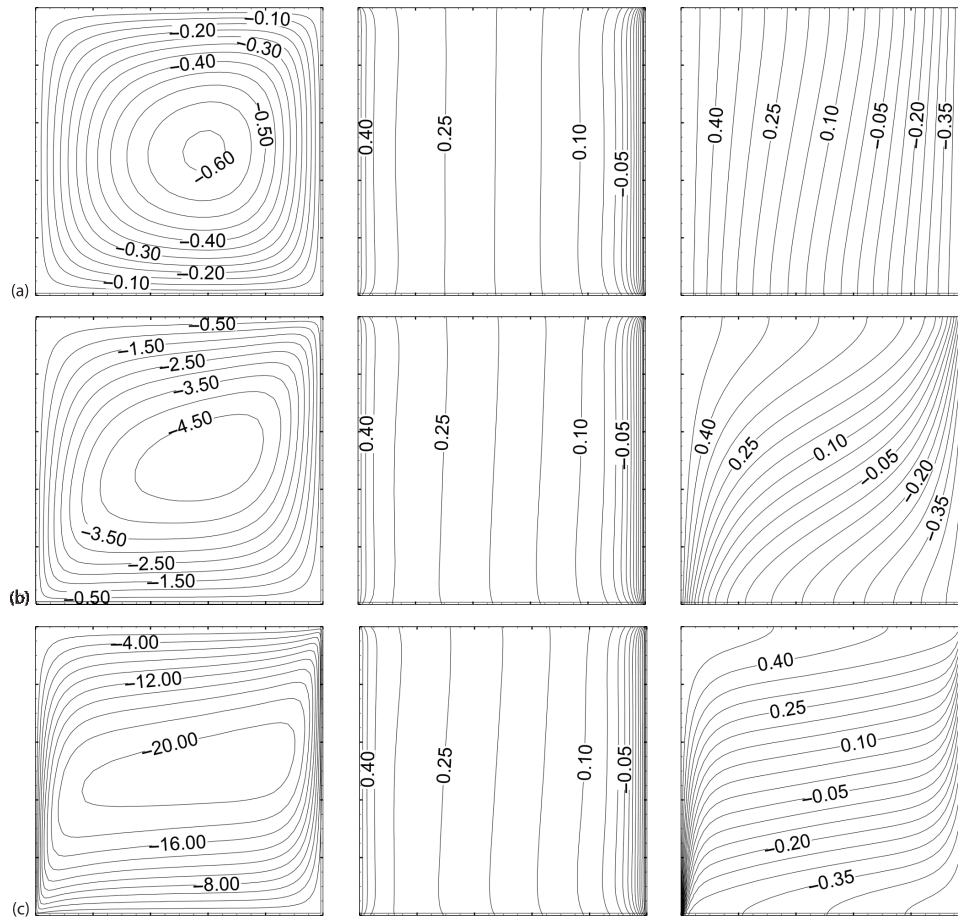


Figure 2. The Ψ (left), θ , (middle) and θ_r (right) for different Rayleigh number with $H = 10$, $\gamma = 1.0$, and $Pr = 0.02$; (a) $Ra = 10$, (b) $Ra = 100$, and (c) $Ra = 1000$

$H = 1$, $H = 10$, and $H = 1000$. Other parameters are kept as $Ra = 1000$, $\gamma = 1.0$, and $Pr = 0.02$. It can be seen that when $H = 0.1$, the fluid circulation cell is almost centrosymmetric in the cavity. At this moment, the convective heat transfer between the two-phases is weak, and the radiative heat transfer has little effect on the fluid phase since it is assumed to be a radiative transparent medium. As H increases, the strength of the fluid-flow is enhanced and accompanied by larger streamline magnitudes. In addition, the cell shifts apparently to the cold wall, thus results in a compression of the streamlines close to this wall. At a lower H , the solid isotherms are almost parallel to the vertical walls; thus, the heat transfer is mostly dominated by radiation and conduction. When H is increased from 0.1-10, the change in the solid isotherms is not obvious. When H increases to 100, the solid isotherms start to twist; as a result, the temperature gradients near the upper cold wall and lower hot wall obviously increase. Due to radiation, the solid isotherms with values over zero occupy most of the space in the cavity. As H increases, the central fluid isotherms move towards both sidewalls, and the average temperature of the fluid in the cavity increases. When H is increased to 1000, the temperature of most fluids in the cavity is higher than zero. Because a higher value of H enhances the heat transfer between

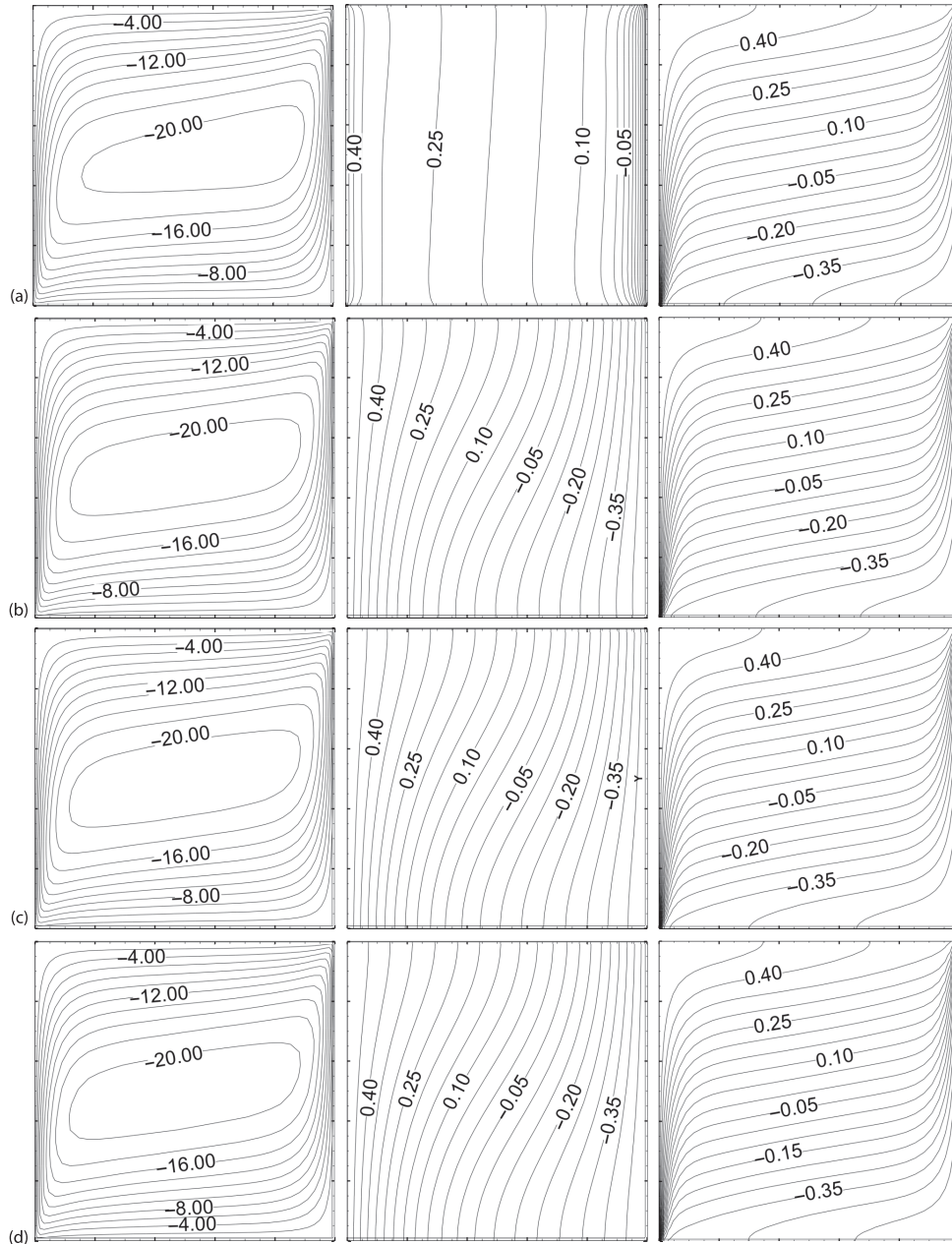


Figure 3. The Ψ (left), θ , (middle) and θ_r (right) for different Rayleigh number with $Ra = 1000$, $H = 10$, and $\gamma = 1.0$; (a) $PI = 0.02$, (b) $PI = 2.0$, (c) $PI = 20$, and (d) without-radiation

the two-phases, when $H = 1000$, the fluid isotherms exhibit a similar distribution with the solid isotherms, which brings their temperatures close to each other until the fluid and solid phases reach the thermal equilibrium state.

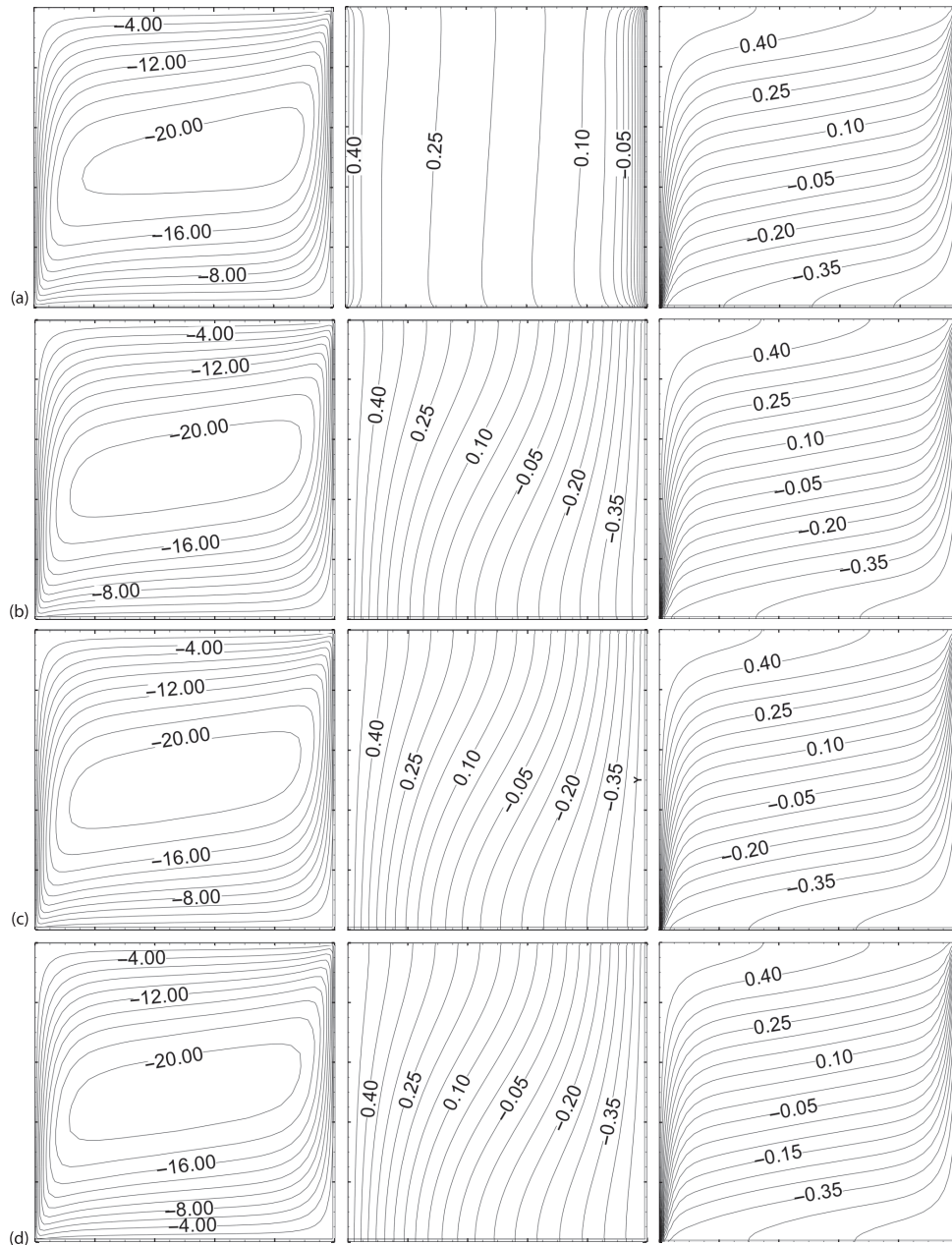


Figure 4. The Ψ (left), θ , (middle) and θ_r (right) for different H with $Ra = 1000$, $\gamma = 1.0$, and $Pl = 0.02$; (a) $H = 0.1$, (b) $H = 1.0$, (c) $H = 10$, and (d) $H = 1000$

Nusselt number

The results of Nusselt number of the hot wall with different parameters are shown in fig. 5. It can be seen that with the increasing of Rayleigh number, the convective Nusselt numbers of the hot wall Nu_h^{COV} increase drastically, while the conductive and radiative Nusselt

numbers of the hot wall $\overline{Nu}^{\text{COD}}$, $\overline{Nu}_h^{\text{R}}$ have not obvious change, meaning the flow in the cavity is strengthened with the increasing of Rayleigh number, while, the thermal field of the solid phase is not sensitive to Rayleigh number, it is still dominated by conduction and radiation. As Planck number increases, only $\overline{Nu}_h^{\text{COV}}$ has a slight increase, both $\overline{Nu}_h^{\text{COD}}$ and $\overline{Nu}_h^{\text{R}}$ decrease. Furthermore, when Planck number larger than 20, $\overline{Nu}_h^{\text{R}}$ is merely 0.0177, which means convection is the dominant mode of heat transfer. As H increases, $\overline{Nu}_h^{\text{COV}}$ decreases sharply, while $\overline{Nu}_h^{\text{COD}}$ and $\overline{Nu}_h^{\text{R}}$ have no significant increments. The reason is that the heat transfer between the two-phases is enhanced with the increasing of H , the difference of the entire thermal field of fluid is evidently reduced due to interaction of the radiation and the convection. Thereby, it can be concluded that increasing H could suppress the overall heat transfer.

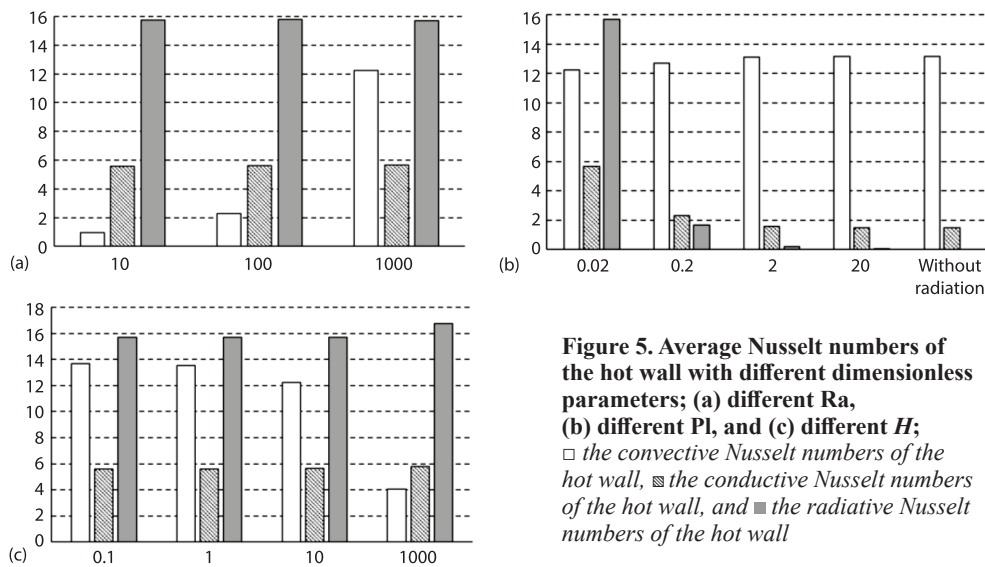


Figure 5. Average Nusselt numbers of the hot wall with different dimensionless parameters; (a) different Ra, (b) different Pl, and (c) different H ;
 □ the convective Nusselt numbers of the hot wall, ▨ the conductive Nusselt numbers of the hot wall, and ■ the radiative Nusselt numbers of the hot wall

Conclusions

A numerical study has been performed on the combined conductive-convective-radiative heat transfer in a porous cavity. Particular effort has been focused on the influence of the radiation. The radiative heat flux distribution in the porous media is computed from the solving of the RTE. The dimensionless stream function, solid/fluid temperature and Nusselt numbers are presented graphically for different values of the crucial parameters. The major findings of the paper are summarized.

- A unicellular fluid cell is found in the porous cavity. Owing to radiation, the cell appears to be asymmetrical. When the Planck number increases to 20, the Ψ and the θ are very similar to those when radiation is not considered. This indicates that the effect of radiation can be neglected when $Pl > 20$.
- Rayleigh number has a significant influence on Ψ and θ_f but little effect on θ_s when the radiation is dominant ($Pl = 0.02$) and the interphase heat transfer is weak ($H = 10$).
- With increasing H , the isotherms of the two-phases (solid and fluid) tend to be similar, which means the recovery of the local thermal-equilibrium can be obtained when H exhibits a very high value, as expected.
- The overall heat transfer of the hot wall increases with the increasing of Rayleigh number, but decreases with the increasing of H and Planck number. The changes of dimensionless

parameters of Rayleigh and Planck numbers have relative great influence on the overall heat transfer.

Acknowledgment

This work was supported by the Natural Science Foundation of China (NSFC) with granted No. 51804234.

Nomenclature

c_p	– specific heat at constant pressure, [Jkg ⁻¹ K ⁻¹]	δ	– overheat ratio
G	– dimensionless incident radiation	ε	– emissivity
g	– gravitational acceleration, [ms ⁻²]	Θ	– dimensionless radiation temperature
H	– inter-phase heat transfer coefficient	θ	– dimensionless temperature in the energy equation
h	– volumetric heat transfer coefficient between solid and fluid, [Wm ⁻³ K ⁻¹]	κ_a	– absorption coefficient, [m ⁻¹]
I	– radiative intensity, [Wm ⁻² Sr ⁻¹]	κ_s	– scattering coefficient, [m ⁻¹]
J	– dimensionless radiative intensity	λ	– conduction coefficient, [Wm ⁻¹ K ⁻¹]
K	– permeability of the porous medium, [m ²]	ν	– kinematic viscosity, [m ² s ⁻¹]
L	– cavity length, [m]	ρ	– density, [kgm ⁻³]
Nu	– Nusselt number	σ	– Stefan-Boltzmann constant, [5.67 · 10 ⁻⁸ Wm ⁻² K ⁻⁴]
\mathbf{n}	– unit outward normal vector of boundary	ζ	– the ratios of thermal diffusivity
Pl	– conduction-radiation interaction parameter	τ_L	– optical thickness
q	– heat flux, [Wm ⁻²]	ϕ	– porosity
Ra	– modified Rayleigh number	Ψ	– stream function
\mathbf{r}	– position vector	$\Omega, \bar{\Omega}$	– solid angle, [Sr]
S	– dimensionless distance travelled by ray	ω	– scattering albedo
s	– distance travelled by ray, [m]		
T	– temperature, [K]	<i>Subscripts</i>	
t	– dimensional time	0	– reference quantities
U	– dimensional velocity in x-direction	b	– black body
u	– velocity in x-direction, [ms ⁻¹]	c	– cold wall
V	– dimensional velocity in y-direction	f	– fluid phase
v	– velocity in y-direction, [ms ⁻¹]	h	– hot wall
X, Y	– dimensional Cartesian co-ordinates	s	– solid phase
x, y	– Cartesian co-ordinates, [m]	W	– wall
		<i>Superscripts</i>	
		COD	– conduction term
		R	– convection term
		COV	– radiation term

References

- [1] Ingham, D. B., Pop, I., *Transport Phenomena in Porous Media III* 2005, Elsevier, Oxford, UK, 2005
- [2] Vafai, K., *Handbook of Porous Media*, 2nd ed., Taylor and Francis, New York, USA, 2005
- [3] Wang, K. Y., Tien, C. L., Thermal Insulation in Flow Systems: Combined Radiation and Convection through a Porous Segment, *Journal of Heat Transfer*, 106 (1984), 2, pp. 453-459
- [4] Nemoda, S., *et al.*, Numerical Simulation of Porous Burners and Hole Plate Surface Burners, *Thermal Science*, 8 (2004), 1, pp. 3-17
- [5] Dupuy, J. L., Larini, M., Fire Spread through a Porous Forest Fuel Bed: a Radiative and Convective Model including Fire-induced Flow Effects, *International Journal Of Wildland Fire*, 9 (1999), 3, pp. 155-172
- [6] Fend, T., *et al.*, Porous Materials as Open Volumetric Solar Receivers: Experimental Determination of Thermophysical and Heat Transfer Properties, *Energy*, 29 (2004), 5-6, pp. 823-833
- [7] Rostamiyan, Y., *et al.*, Analytical Investigation of Non-linear Model arising in Heat Transfer through the Porous Fin, *Thermal Science*, 18 (2014), 2, pp. 409-417

- [8] Darvishi, M. T., et al., Unsteady Thermal Response of a Porous Fin under the Influence of Natural-Convection and Radiation, *Heat and Mass Transfer*, 50 (2014), 9, pp. 1311-1317
- [9] Astanina, M. S., et al., Effect of Thermal Radiation on Natural-convection in a Square Porous Cavity Filled with a Fluid of Temperature-dependent Viscosity, *Thermal Science*, 22 (2018), 1, pp. 391-399
- [10] Sheikholeslami, M., Shehzad, S. A., Magneto-hydrodynamic Nanofluid Convection in a Porous Enclosure considering Heat Flux Boundary Condition, *International Journal of Heat and Mass Transfer*, 106 (2017), Nov., pp. 1261-1269
- [11] Shateria, A. R., Salahshour, B., Comprehensive Thermal Performance of Convection-Radiation Longitudinal Porous Fins with Various Profiles and Multiple Non-Linearities, *International Journal of Mechanical Sciences*, 136 (2018), Feb., pp. 252-263
- [12] Chen, H., et al., Least Square Spectral Collocation Method for Non-Linear Heat Transfer in Moving Porous Plate with Convective and Radiative Boundary Conditions, *International Journal of Thermal Science*, 132 (2018), Oct., pp. 335-343
- [13] Ghalambaz, M., et al., Free Convection in a Square Cavity filled by a Porous Medium Saturated by a Nanofluid: Viscous Dissipation and Radiation Effects, *Engineering Science and Technology an International Journal*, 19 (2016), 3, pp. 1244-1253
- [14] Jamal-Abad, M. T., et al., Heat Transfer in Concentrated Solar Air-heaters Filled with a Porous Medium with Radiation Effects: A Perturbation Solution, *Renewable Energy*, 91 (2016), June, pp. 147-154
- [15] Lopez, A., et al., Entropy Generation Analysis of MHD Nanofluid-Flow in a Porous Vertical Micro-Channel with Non-Linear Thermal Radiation, Slip Flow and Convective-radiative Boundary Conditions, *International Journal of Heat and Mass Transfer*, 107 (2017), Apr., pp. 982-994
- [16] Barnoon, P., et al., Two-Phase Natural-Convection and Thermal Radiation of Non-Newtonian Nanofluid in a Porous Cavity Considering Inclined Cavity and Size of Inside Cylinders, *International Communications in Heat and Mass Transfer*, 108 (2019), 104285
- [17] Arafa, A. A. M., et al., Radiative Flow of Non-Newtonian Nanofluids within Inclined Porous Enclosures with Time Fractional Derivative, *Scientific Reports*, 11 (2021), 5338
- [18] Ajibade, O. A., et al., Effects of Dynamic Viscosity and Non-linear Thermal Radiation on Free Convective Flow through a Vertical Porous Channel, *International Journal of Thermofluids*, 9 (2021), 100062
- [19] Olajuwon, I. B., Convection Heat and Mass Transfer in a Hydromagnetic Carreau Fluid past a Vertical Porous Plate in Presence of Thermal Radiation and Thermal Diffusion, *Thermal Science*, 15 (2011), 2, pp. 241-252
- [20] Izadi, M., The MHD Thermogravitational Convection and Thermal Radiation of a Micropolar Nanoliquid in a Porous Chamber, *International Communications in Heat and Mass Transfer*, 110 (2020), 104409
- [21] Talukdar, P., et al., Combined Radiation and Convection Heat Transfer in a Porous Channel Bounded by Isothermal Parallel Plates, *International Journal of Heat and Mass Transfer*, 47 (2004), 5, pp. 1001-1013
- [22] Abdesslem, J., et al., Radiative Properties Effects on Unsteady Natural-Convection Inside a Saturated Porous Medium: Application for Porous Heat Exchangers, *Energy*, 61 (2013), C, pp. 224-233
- [23] Elgazery, N. S., An Implicit-Chebyshev Pseudospectral Method for the Effect of Radiation on Power-Law Fluid Past a Vertical Plate Immersed in a Porous Medium, *Communications in Non-linear Science and Numerical Simulation*, 13 (2008), 4, pp. 728-744
- [24] Chen, X., et al., Transient Thermal Analysis of the Coupled Radiative and Convective Heat Transfer in a Porous filled Tube Exchanger at High Temperatures, *International Journal of Heat and Mass Transfer*, 108 (2017), PB, pp. 2472-2480
- [25] Mahmoudi, Y., Effect of Thermal Radiation on Temperature Differential in a Porous Medium under Local Thermal Non-Equilibrium Condition, *International Journal of Heat and Mass Transfer*, 76 (2014), Sept., pp. 105-121
- [26] Mesgarpour, M., Numerical Optimization of a New Concept in Porous Medium considering Thermal Radiation: Photovoltaic Panel Cooling Application, *Solar Energy*, 216 (2021), 5, pp. 452-467
- [27] Raptis, A., Radiation and Free Convection Flow through a Porous Medium, *International Communications in Heat and Mass Transfer*, 25 (1998), 2, pp. 289-295
- [28] Chen, Y. Y., et al., Influences of Radiative Characteristics on Free Convection in a Saturated Porous Cavity under Thermal Non-Equilibrium Condition, *International Communications in Heat and Mass Transfer*, 95 (2018), July, pp. 80-91
- [29] Baytas, A. C., Pop, I., Free Convection in a Square Porous Cavity using a Thermal Non-equilibrium Model, *International Journal of Thermal Science*, 41 (2002), 9, pp. 861-870

- [30] Chen, S. S., *et al.*, Chebyshev Collocation Spectral Method for Solving Radiative Transfer with the Modified Discrete Ordinates Formulations, *International Journal of Heat and Mass Transfer*, 88 (2015), Sept., pp. 388-397
- [31] Manole, D. M., Lage, J. L., Numerical Benchmark Results for Natural-Convection in a Porous Medium Cavity, *Proceedings*, HTD-Vol. 216, Heat and Mass Transfer in Porous Media, ASME Conference, 1992, Anaheim, Cal., USA, pp. 55-60
- [32] Moya, S. L., *et al.*, Numerical Study of Natural-Convection in a Tilted Rectangular Porous Material, *Int. J. Heat Mass Transfer*, 30 (1987), 4, pp. 741-756